Memoria de Investigación
Programa de doctorado del Departamento de Física.
Bienio 1995-1997

STOCHASTIC RESONANCE IN THE THERMOHALINE CIRCULATION

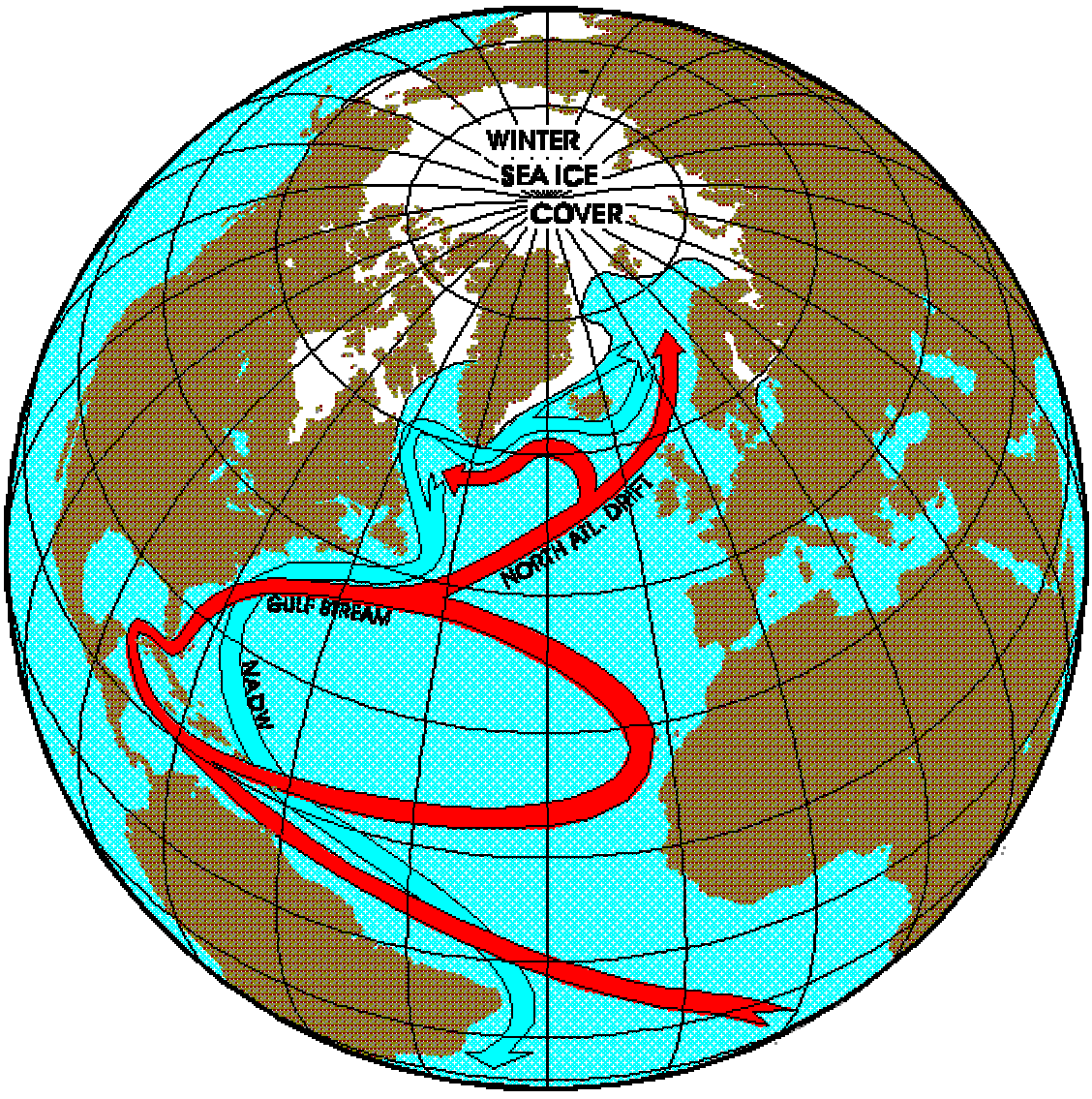

Pedro Joaquín Vélez Belchí
Departamento de Física
Universidad de Las Islas Baleares

INDEX

Agradecimientos:

A Joaquín Tintoré, por iniciarme en el hermoso mundo de la oceanografía. A Alberto Álvarez, por darme a conocer los secretos de la *lógica difusa.* A Pere Colet, por enseñarme los misterios del *ruido*. A Bob Haney, de la Naval Postgraduate School (EEUU), por desvelarme los misterios de la dinámica oceánica. A los miembros del departamento de Física, del grupo de oceanografía física y del grupo de física no-lineal de la Universidad de las Islas Baleares. A Benjamín Casas, Vicente Fernández, Marga Riera, Jean-Michel Pinot, Rafael Gallego, Fabrice Ardhuin, Esther Asencio, Miguel Curbelo, habitantes de la *Agencia Efe*..., que me ayudaron de manera incondicional durante todos estos años y sin los cuales el presente trabajo no hubiera llegado a buen puerto.

De manera especial agradezco a mi familia, a mis amigos, a Ana y a Belén, que me animaron y apoyaron en todo momento.

A las dos Instituciones que han hecho posible la realización de este trabajo: el Ministerio de Educación y Ciencia por la beca FPI (FP95 43790142) que me permitió realizar el programa de doctorado en la Universidad de las islas Baleares, así como estancias en la Naval Postgraduate School de Monterey (California, EEUU); y el Instituto Español de Oceanografía, que me apoyo para poder finalizar este trabajo y continuar los estudios de doctorado.

Cover Figure

Thermohaline circulation in the north Atlantic, the red arrow shows the warm surface waters, while the blue one shows the path of the North Atlantic deep waters [Adapted from Rahmstorf 1995].

Abstract

A wide variety of climate records have revealed the existence of sudden a recurrent climatic changes in the past. An important part of this variability might be related to transitions between stable equilibrium states of the thermohaline circulation. Here, we employ a box model of the ocean thermohaline circulation to show that in the presence of environmental fluctuations, a subthreshold periodic perturbation in the fresh water fluxes can induce quasiperiodic transitions between the stable states of the thermohaline circulation. This enhanced response occurs for a wide range of frequencies, including the Milankovic orbital forcing, and amplitudes. The mechanism that allows such response of the system under small perturbations arises from a non-linear cooperation between the periodic perturbations and the fluctuations. Through this nonlinear mechanism, called stochastic resonance, significant climatic variability may be originated due to small perturbations enhanced by environmental noise and dynamics.

Motivation

The earth climate is a complex system formed by many interacting components, where a set of important phenomena arise from the interaction between different spatial-temporal scales. Scales ranging from centimetres to thousands of kilometres and from seconds to thousands of years. The interaction between scales is consequence of the nonlinear character of the equations that govern fluid dynamics, in particular, the advective term ($\vec{u} \cdot \nabla \vec{u}$) in the Navier-Stokes equations. This interaction makes possible the existence of large-scale processes controlled by small-scale ones.

In the climate system, the role played by the ocean is as important as the one played by the atmosphere, since in average, the ocean and the atmosphere transport almost equal amounts of heat (see fig. 1). Being the thermohaline circulation the most important component, in a climate sense, of the ocean circulation. In summary, understanding the cascade of energy from the small-scale processes to the large-scale behaviour of the ocean is a key point in the understanding of the climate variability. The present work has been focused in this topic, specifically in the influence of small-scale processes in the large-scale thermohaline ocean circulation.

We propose a mechanism called stochastic resonance (hereinafter SR) that is able to induce coherent transitions between the stable states of the thermohaline circulation (hereinafter THC), enhanced by the presence of environmental noise. The scope of this study is to show that SR is a mechanism of variability, for a wide range of periods, in the dynamical behaviour of the THC and therefore in certain aspects of climate variability.

1 Introduction

The THC is that part of the global ocean circulation driven by large-scale density differences. These density differences are ultimately governed by heat and freshwater fluxes at the ocean surface, being the air/sea interaction fundamental in governing the THC. The present-day THC (Gordon, 1986) is characterised by deep-water formation in the North Atlantic (by convection in the Norwegian and Labrador Sea). The deep water is formed when, under prevailing conditions of high surface density, weather conditions are able to low enough the superficial temperature to produce an unstable situation with heavier water on top of lighter water. Under such unstable situation, the water at the surface sinks until it reaches the equilibrium depth, around 3000m for the deep waters formed in the North Atlantic. The observed higher salinity, and therefore density, of the northern Atlantic is maintained by the enhanced evaporation rate due to the warmer surface waters that are brought as compensation flow to the deep water being formed in the North Atlantic. The system thus provides itself with the high North Atlantic density necessary to form North Atlantic deep waters (hereinafter NADW).

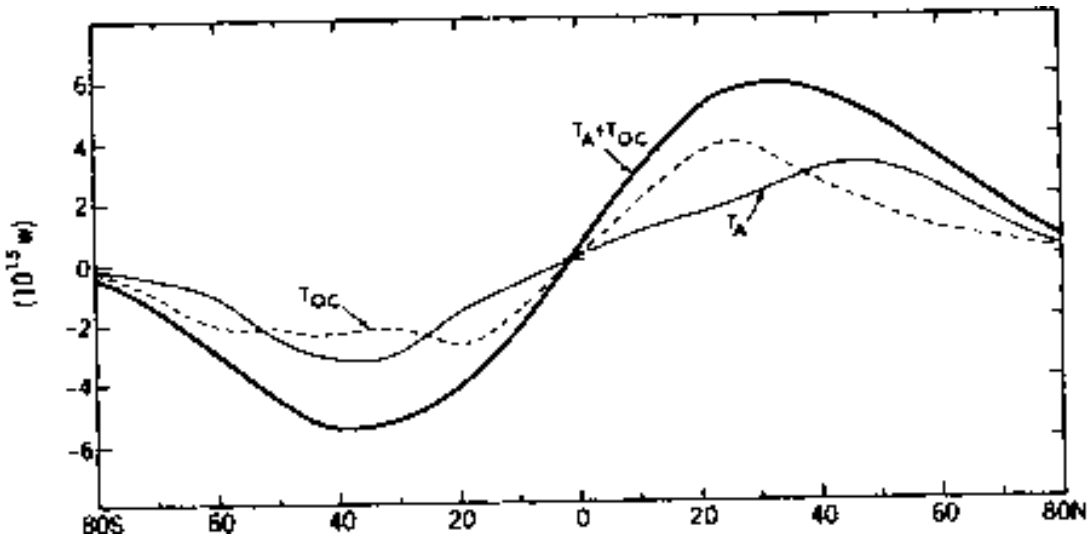

Figure 1. Annual mean meridional heat transport, in the ocean and in the atmosphere, in units of PW (1PW=10^{15}W) [From Peixoto and Oort (1992)].

After formation, the deep water moves southward, at a depth of 2-3 Km, across the equator and joins the circumpolar current on its path to the Indian and Pacific Ocean, where it upwells. The upwelled water stays as termocline water on its way back to the Indian Ocean, storing heat and hence moving up to the surface while crossing the Mozambique channel back to the North Atlantic. This circulation pattern provides the dominant transport of heat in the ocean and has a large influence on the distribution of surface temperatures. On annual average, warm near-surface water crosses the equator northward in the Atlantic, causing a cross-equatorial volume transport of about 17 Sv, with an associated heat transport between 0.5×10^{15} W and 1.5×10^{15} W (Roemmich and Wunsch, 1985; Gordon, 1986; Parrilla et al., 1994). This transport, see fig.1 and 2, is due to the difference between the temperature of the NADW and the temperature of the waters that reach the North Atlantic, around 20ºC. The transport can be easily estimated as follows:

$$\textit{Heat transported} = \text{volume transport} \times (T_{final} - T_{initial}) \times C_w \times \rho_0 =$$
$$= 17 \times 10^6\ m^3 s^{-1} \times 20ºC \times 4000\ J\ ºC^{-1} kg^{-1} \times 1027\ kg m^{-3} = 1.40 \times 10^{15} W =$$
$$1.40 pW\ (petaWatts)$$

Where C_w is the specific heat capacity of seawater and ρ_0 a mean sea-water density.

This heat transport, representing 30 % of the solar heat reaching the surface of the Atlantic within the region north of 35ºN, has a strong impact on the climate of Europe. As result of this transport the Atlantic is kept, on average, 4ºC warmer than the Pacific (Levitus, 1982). Another important characteristic of the THC, see fig. 2, is the anomalous heat transport of the Atlantic ocean, that transports heat northward at all latitudes, unlike the Pacific and Indian oceans which move heat from the tropics to high latitudes in both hemispheres.

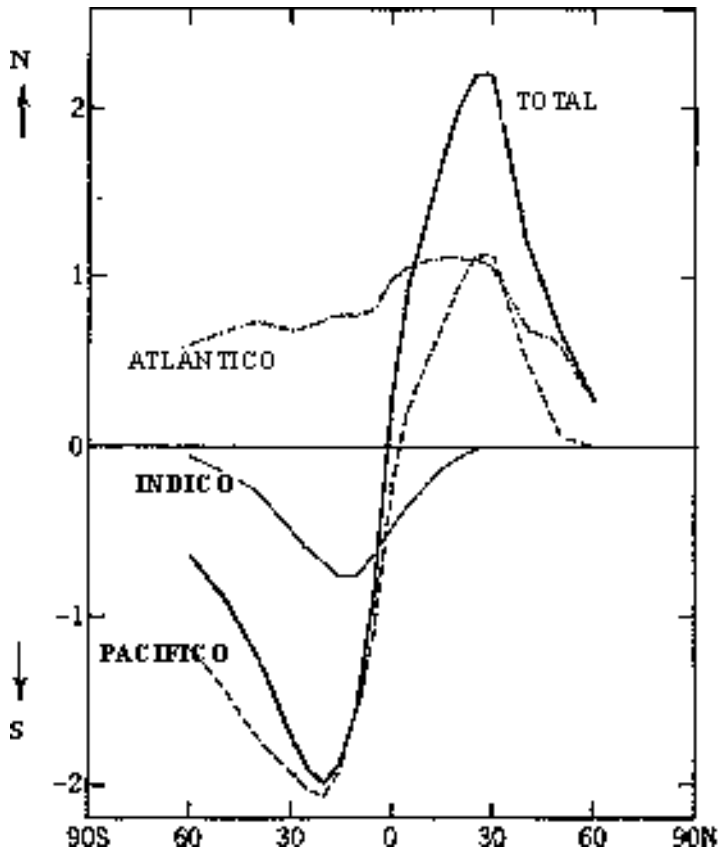

Figure 2. Annual mean meridional heat transport in the different ocean basins in units of PW (1PW=10^{15}W).[From Peixoto and Oort (1992)]

1.1 Bistability

The heat transported by the THC largely determines important aspects of the Earth's climate (Bond, 1995; Dansgaard et al., 1993). The important role played by the THC regulating the climate has allowed to establish a link between past climate changes and the dynamical behaviour of the THC. Specifically, recent experimental studies (Ditlevsen, 1999), using calcium signal from a 110 kyrs Greenland ice-core as climate proxy, have shown that the climate, and therefore the THC, can be represented by a double-well potential dynamical system. The two wells representing the warm interglacial state and the cold glacial state. Numerical models have also confirmed this multiple equilibrium property of the THC (Stommel, 1961; Bryan, 1986; Marotzke and Willebrand, 1991; Thual and McWilliams, 1992; Cessi, 1994; Hughes and Weaver, 1994; Rahmstorf, 1995). Besides the intrinsic nonlinear nature of the THC, climate records show that the THC has also been subjected to the effects of external environmental fluctuations (Bond, 1995; Ditlevsen, 1999).

The different coupling of the temperature and salinity oceanic fields to the atmosphere is a crucial ingredient to explain the existence of multiple stable equilibrium states in the THC. Since the surface heat flux strongly depends on the sea surface temperature (SST), SST anomalies are rapidly removed by enhanced heat gain or loss. On the other hand, the surface salinity has negligible influence on the evaporation and precipitation rates, and therefore the surface salinity anomalies can persist on much longer scales. The different time scale for the interaction with the atmosphere for the heat and freshwater exchange and the fact that the saline and thermal torque works in opposite directions (in the density equation) make possible bistability in the long scale flows. The mechanism is the following: at low flows, the long time scale of the salinity anomalies works against the thermal torque carrying the system to a steady state haline dominated. In contrast, strong flows are dominated by the thermal forcing.

In summary, we have shown the importance of the THC as part of the climate system, being the air/sea interaction at the deep water formation places the key factor controlling the large scale THC. Paleoclimatic data and models have shown that the THC can be seen as a nonlinear bistable system embedded in a fluctuating environment, with climatic variability originated by fast flip-flop between the steady states of the THC. These flip-flops could be produced by changes in the atmospheric forcing (Dansgaard et al., 1993; Kennet and Scott, 1991). Climate records also show fluctuations in the rate of formation of NADW (Bond 1995; Bond et al., 1993), indicating that the THC has also been subjected to the effects of environmental fluctuations. In other words, the THC can be seen as a bistable system embedded in a fluctuating environment. Nonlinear systems characterised by a bistable nature show a rich physical behaviour in the presence of noise. One of the characteristic phenomena related to that sort of systems is called stochastic resonance. The basic idea underlying SR is that the fluctuation induced transitions between the stable states of the nonlinear system can be synchronised by very weak periodic forcing yielding a strong enhancement of the system response. This synchronisation generates a noise induced enhancement of the response of the climatic system.

The main goal of this work is to propose SR as a possible mechanism able to generate the observed transitions in the THC. To test the hypothesis of SR in the THC it seems reasonable to look for a model that is as simple as possible, but that is also able to capture the main aspects of its nature, especially its bistable character. The simplest models for this purpose are the well-known box models (Stommel, 1961; Rooth, 1982; Cessi, 1994) which represent the coarsest possible

general circulation models (GCM) of the ocean. These simple models allow us to discriminate between the different mechanisms that force the THC and test ideas that would need enormous amount of computation time to be tested in full GCMs. Atmospheric versions of such box models are the Energy Balanced Models that allowed the discovery of the ice-albedo feedback and its consequence in the ice-ages (Benzi et al., 1982; review is given in Ghill and Childress, 1987). To study SR in a simple context, we have chosen the model developed by Cessi (1994).

The remainder of the present work is organised as follows: in section 2, we describe the model used to study the existence of SR. In section 3, the SR mechanism is described. Section 4 shows the numerical experiments carried out with the model. Finally, in section 5 some discussion is introduced and the conclusions are presented. Section 6 includes some ideas for future studies.

2 The model

There are a number of mathematical theories that models the THC based on approximations of the Navier Stokes equations similar than those used in the wind-driven circulation theory. All of these theories are phenomenological in the sense that the main forcing of the THC is parameterised in terms of the rate of deep-water formation in a given place. In other words, these theories provide a geographical picture of the deep currents system that forms the THC, but they do not say anything about the role that the air/sea interaction plays in controlling the strength of the THC. However, we have chosen a box model similar to the one developed by Stommel, where the two main forcings that act over the THC are included. Cessi (1994) modified the exchange function (the one that controls the flow between the boxes) in the Stommel model and used a quadratic one, based on a study of the behaviour of a 2-D boussinesq model.

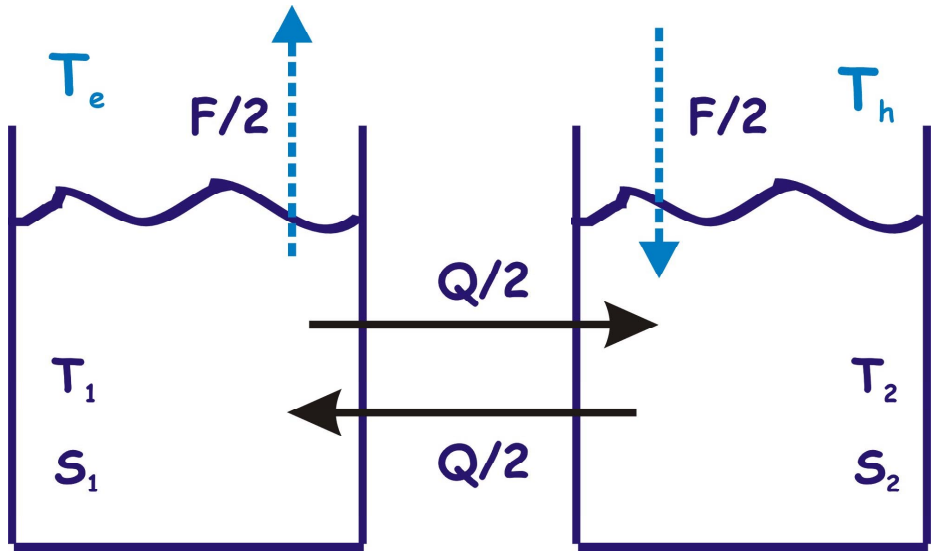

Figure 3. The two box model for the ocean thermohaline circulation. Box 1 (the low-latitude warm water) has a temperature $T_1(t)$ and box 2 (the high-latitude cold water) has a temperature $T_2(t)$. The salinities are $S_1(t)$ and $S_2(t)$, respectively.

The model is a two box model, see fig. 3, consisting of a high latitude box (box 2) and a low latitude box (box 1), that model the vertically averaged circulation in a single hemisphere. This division of the basin in two boxes is based on the differential North/South solar heating and freshwater flux. The temperatures and salinities are labelled with the box number ($T_{1,2}$ and $S_{1,2}$). The equation of state used is a linear approximation around the value ρ_0=1029 kg/m^3, with T_0=5ºC and S_0=35psu:

$$\rho = \rho_0 + \alpha_s (S - S_0) - \alpha_T (T - T_0) \ ,$$

with coefficients α_t=0.171 Kg m^{-3}/ºC, α_s =0.781 Kg m^{-3}/psu.

The temperature and salinity equations that govern the box model are the following:

$$\begin{aligned}
\frac{dT_1}{dt} &= -t_r^{-1} (T_1 - T_e) - \tfrac{1}{2} Q (T_1 - T_2) \\
\frac{dT_2}{dt} &= -t_r^{-1} (T_2 - T_h) - \tfrac{1}{2} Q (T_2 - T_1) \\
\frac{dS_1}{dt} &= \tfrac{1}{2} F S_0 - \tfrac{1}{2} Q (S_1 - S_2) \\
\frac{dS_2}{dt} &= -\tfrac{1}{2} F S_0 - \tfrac{1}{2} Q (S_2 - S_1)
\end{aligned} \qquad (1)$$

The second terms on the right hand sides represent the transport of heat and salt between the boxes, while the first terms represent the air-sea interaction for which mixed boundary conditions are used. Mixed boundary conditions are an essential component in a model that is designed to capture the main characteristics of the THC. Temperature is forced by a Newtonian restoring condition, which parameterise the heat transfer from the atmosphere, using a time scale of t_r equal for both boxes, and relaxation temperatures T_h and T_e for high and low latitude boxes, respectively. Salinity forcing consists of atmospheric vapour transports, converted to an equivalent salt transport multiplication by -S_0, where S_0=35 psu is a fixed reference salinity. We only consider the effect of freshwater forcing, *F*, on salinity, neglecting its effect on the mass balance.

The boxes are assumed to be well mixed and convective mixing is not explicitly parameterised. In this case the exchange function between the boxes can be written as:

$$\begin{aligned} Q &= \frac{1}{t_d} + \frac{(\alpha_t\,(T_e - T_h))^2}{t_a}(\Delta\rho)^2 \\ \Delta\rho &= \alpha_s\,(S_1 - S_2) - \alpha_T\,(T_1 - T_2)\ , \end{aligned} \tag{2}$$

after Cessi and Young (1992) and Cessi (1994), where $\Delta\rho=\rho_1-\rho_2$ is the difference in density between boxes. In (2) t_d is a diffusive scale and t_a represents the advective time scale.

The bistable character of the THC is well represented in this box model. When Q is relatively large, the evaporation/precipitation is unimportant because the fluid parcels do not reside in each box long enough for these processes to be significant. In this case, the thermal forcing dominates and the flow is thermally driven. In cases where Q is relatively small, the ocean has plenty of time to get its superficial temperature equal to the equilibrium temperature of the atmosphere, and evaporation/precipitation processes have enough time to modify S_1 and S_2. In such a situation, the salinity forcing cancels out the thermal forcing and the flow is salinity driven.

2.1 Nondimensional equations

The four equations (1) are not independent and therefore the system can be simplified by subtracting the equations. This gives a pair of coupled equations for salinity and temperature differences between the boxes:

$$\begin{aligned} \frac{d\Delta T}{dt} &= -\frac{1}{t_r}(\Delta T - \Delta T^*) - Q\,\Delta T \\ \frac{d\Delta S}{dt} &= F - Q\,\Delta S\ , \end{aligned} \tag{3}$$

where $\Delta S = S_1 - S_2$, $\Delta T = T_1 - T_2$ and $\Delta T^* = T_e - T_h$.

The model equations (2) and (3) can be written in nondimensional form. The variables are scaled using the natural scale for them: diffusive time for time, high-low latitude temperature differences for temperature and the value of ΔS when the density difference becomes zero, using the high-low latitude temperature differences, for salinity,

$$x = \frac{\Delta T}{\Delta T^*},\ y = \frac{\alpha_s \Delta S}{\alpha_t \Delta T^*}\ , \tau = \frac{t_d}{t}$$

Using these new variables the model becomes:

$$\begin{aligned} \dot{x} &= -\alpha (x - 1) - x \left[1 + \mu^2 (x - y)^2\right] \\ \dot{y} &= p - y \left[1 + \mu^2 (x - y)^2\right], \end{aligned} \tag{4}$$

where the dot means derivative with respect to the nondimensional time τ and

$$\alpha = \frac{t_d}{t_r}, \ \mu^2 = \frac{t_d}{t_a}, \ p = \frac{\alpha_s S_0 t_d F}{\alpha_t \Delta T^*}.$$

Note that $q=1+\mu^2(x-y)^2$ is the nondimensional transport function.

2.2 Parameters

In order to have the thermohaline circulation correctly represented by the box model, an appropriate set of parameters should be chosen. A typical value for the diffusion time t_d is about 219 years. The relaxation time scale for temperature has been chosen as t_r=220 days, ten times bigger than the value used by Cessi (1994). This change is based on the work by Rahmstorf and Willebrand (1995), where the restoring condition for the heat exchange with the atmosphere on large spatial scales has been revised. As result, the role of the atmosphere is a negative feedback rather than an almost constant sink of heat. With this t_r, the value of α is 3.6×10^2. The difference in air temperature between high and low latitude has been chosen as ΔT^*=20ºC. The western boundary current determines the advective time scale. The present-day North Atlantic transport is ≈17Sv (Roemmich and Wunsch, 1985). We can estimate the transport volume as V= L H W, where H≈ 4500 m is the average depth, L≈8220 km is the north-south scale and W≈500km is the width of the western boundary current. These values yield an advective time $t_a \approx$ 35yr and therefore μ^2=6.25. The mean freshwater flux into the North Atlantic, $\overline{F}$, is about 2.3m/yr ≈ 7.3×10^{-4} yr^{-1} (Schmitt et al., 1989) and therefore $\overline{p}$=1.1.

2.3 Time-depend freshwater fluxes

In principle, the thermal forcing is less possible to change, due to its origin, therefore the role that play the freshwater fluxes is crucial to understand the present and past of the THC. Freshwater over the Atlantic can be seen as a breaking/driving mechanism of the THC. To investigate SR in the previously described box model, we consider the forcing by the freshwater flux to be time-dependent:

$$p(\tau) = \bar{p} + A \sin(\omega\tau) + \sqrt{\varepsilon}\,\chi(\tau), \tag{5}$$

The first term on the right hand side is the mean value, the second is a periodic forcing with amplitude A and period $T=2\pi\omega$. The last term $\sqrt{\varepsilon}\chi(\tau)$ is noise. In particular, it has been taken $\chi(\tau)$ to have a Gaussian distribution with zero mean:

$$\langle \chi(\tau) \rangle = 0, \tag{6a}$$

and correlation:

$$\langle \chi(\tau)\chi(\tau') \rangle = 2\delta(\tau - \tau'), \tag{6b}$$

where $\delta(\tau - \tau')$ is the Dirac delta. This kind of noise is called Gaussian white noise.

This periodic forcing represents weak variations of fresh water fluxes with certain periodic component, like the precipitation changes over the North Atlantic induced by the Milankovic rhythms (Adams et al., 1999). The noise term models perturbations that occur with time scales much smaller than the characteristic time scale of the system.

2.4 Steady states

In order to examine the distribution of steady state solutions, (4) was solved for $\dot{x} = \dot{y} = 0$ with a constant value for p, yielding the following equation for the steady-state value of the nondimensional transport $q_s=1+\mu^2(x-y)^2$,

$$0 = 1 + \mu^2 \left[\frac{\alpha}{\alpha + q_S} - \frac{p}{q_S} \right]^2 - q_s$$

the steady-state values for salinity and temperature differences, y_s and x_s respectively, can be obtained from q_s as:

$$y_s = \frac{p}{q_s} \quad , \quad x_s = \frac{\alpha}{\alpha + q_s}.$$

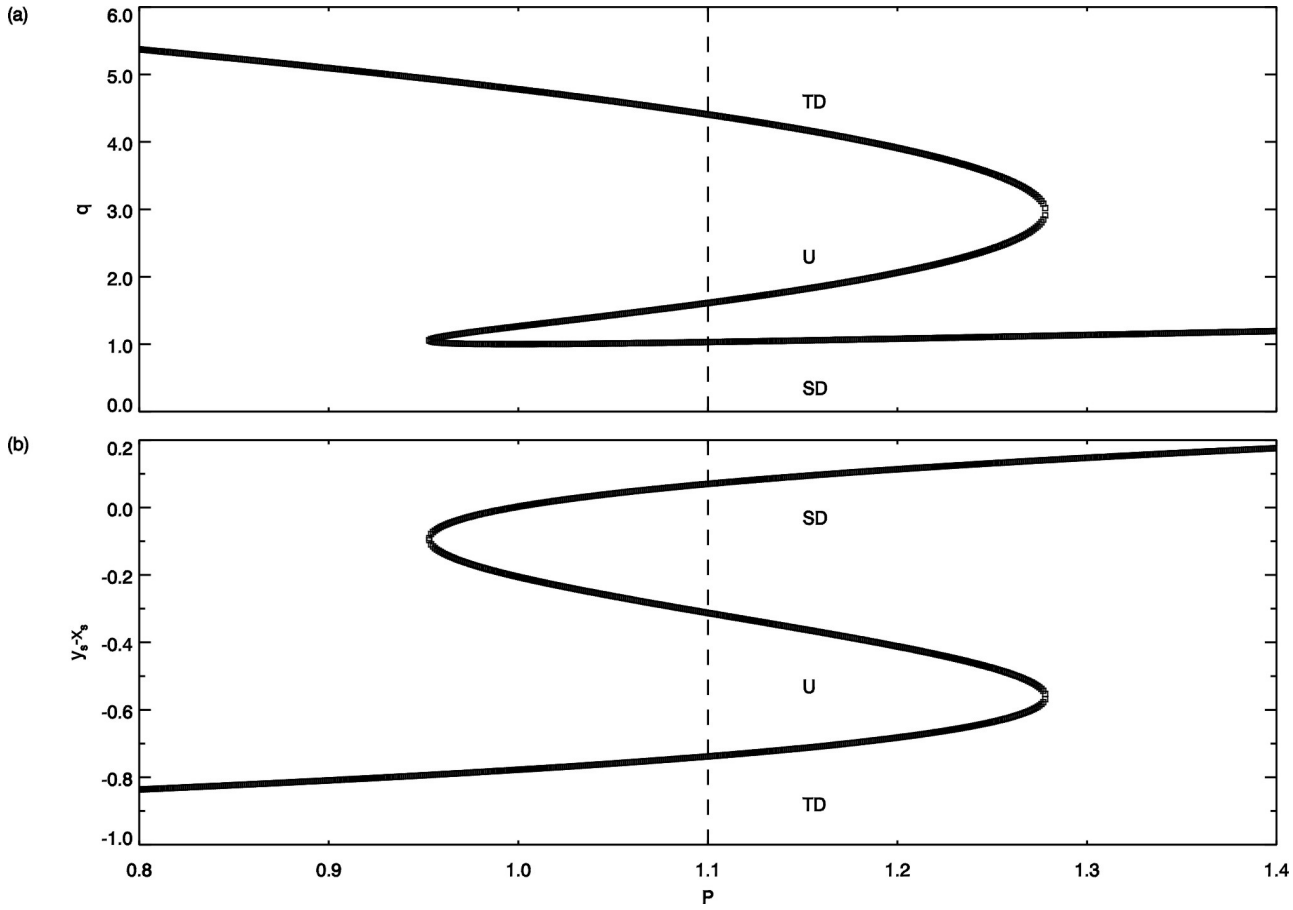

Figure 4. (a) Steady-state nondimensional transport (q_s) for the two box model using α=3.6x10^2 and μ^2=6.25. The x-axis represents the control parameter p, which is related to the freshwater flux. The three branches found are labelled as TD (thermally driven), U (unstable) and SD (salinity driven). (b) Same as (a) except for the nondimensional density difference y_s-x_s. The branches are labelled in the same way as in (a)

Fig. 4 shows the steady states for the system using the values for α and μ^2 given in the previous section. The horizontal axis represents the control parameter p (related to the freshwater forcing) and the vertical axis the steady-state nondimensional transport q_s and the density difference (y_s-x_s). Note that y_s-x_s<0 corresponds to $\Delta\rho_s$<0, which means the more buoyant water is the low latitude box. We have obtained a hysteresis curve, characteristic of a bistable system, with two saddle node points as found in classical studies (Stommel, 1961). The states on the upper branch (labelled TD, thermally driven) are states with stronger transport of heat (QΔT) and salt (QΔS) from the equator towards higher latitudes, and can be associated with the present-day circulation, i.e. with strong NADW formation. The states on this branch are thermally driven since the thermal contribution to $\Delta\rho$ is bigger than the salinity one. On the other hand, the states on the lower branch (labelled SD, salinity driven) are states with weaker transport of heat and salt towards higher latitudes and could be associated with the circulation in some periods of the past characterised by weak NADW formation. The states on this branch are salinity driven since the salinity contribution to $\Delta\rho$ is bigger than the thermal contribution. It is important to note that even when the density difference y_s-x_s is positive, with the more buoyant water in the high latitude box 2 (fig. 4b), the transport function, q_s, is positive (fig. 4a). This is consistent with the vertically averaged character of the model, where Q must be always seen as heat transport QΔ T and salt transport QΔ S. Both have to be positive since the heat and salt are transported from low towards high latitudes by the THC. Thus, it is more appropriate to say that the box model represent the transport of the THC rather than the particular directions of the currents.

In the region bounded by 0.95<p<1.28, the TD and SD branches coexist, and are connected through an unstable branch (labelled as U). Starting from an arbitrary initial condition, and without the effect of the noise, the system will always reach one of the stable steady solutions. Beyond the critical value of p_c>1.28, the system is no longer bistable, since only the weaker state exits. In this situation, the salinity forcing is bigger than the thermal forcing and therefore, the system is now salinity driven, unlike the present-day circulation that is thermally driven. For p_c<0.95 only the strong circulation state remains.

3 Physical description of the stochastic resonance mechanism

In this section we present and describe the mechanism of SR using a potential version of the equations that define the model. Some of the aspects presented here are well known in areas such as statistical physics. However, since they are quite uncommon in physical oceanography, we have included them for completeness.

The basic idea underlying SR is that noise induced transitions between the stable states of the nonlinear system can be synchronised by very weak periodic forcings, yielding a strong enhancement of the system response (Benzi et al., 1981, 1982). Specifically, bistable systems can be described by a potential with two stable states, separated by a potential barrier. In the absence of any external forcing, the system will remain in one of the two stable states. If the bistable system is forced by noise, transitions between the two equilibrium states will occur on a mean escape time T_M (Gardiner, 1985). On the other hand, if the bistable system is forced by a periodic forcing, the system response will depend on the amplitude and frequency of the forcing. In case the periodic forcing is too weak to cause the system to scale the potential barrier, it will remain oscillating in the neighbouring of the initial stable state. Such weak forcing is denominated sub-threshold. For forcings strong enough to overcome the potential barrier that separate the two stable states, transitions will occur between the two states with the same period of the forcing, T_O. The phenomenon of SR appears when the bistable system is driven by both, an additive random noise, for simplicity white and Gaussian, and a sub-threshold periodic forcing. The weak periodic forcing modulates in time the height of the potential barrier, changing the mean escape time. A tuning of the forcing period T_O and the mean escape time T_M can result from this process. Then, the system will show transitions between the two stable states with the same period T_O of the weak forcing and in phase with it (reviews on SR are given in Wiesenfeld and Moss, 1995).

3.1 Potential

Under the assumption of $\alpha >> 1$, the fast variable can be adiabatically eliminated from the dynamical equations and keep fixed at the value x=1. As result, the system will be described only by the nondimensional salinity difference y:

$$\dot{y} = p(\tau) - y\left[1 + \mu^2 (1 - y)^2\right] . \tag{7}$$

This equation describes the motion of a particle with damping and without inertia in the following double welled pseudo-potential:

$$V(y) = \frac{y^2}{2} + \mu^2\left[\frac{y^4}{4} - \frac{2y^3}{3} + \frac{y^2}{2}\right] - p(\tau)y\,, \qquad \dot{y} = \frac{\partial V}{\partial y} \tag{8}$$

The potential, see fig. 5, is characterised by two minima, corresponding to the stable steady states, and a maximum, which corresponds to the unstable steady state. The minimum with the larger y value represents the weak THC circulation (denoted W), while the minimum with the smaller y value represents the present-day strong THC circulation (denoted S). Without any external forcing, friction will cause the system to settle down near the bottom of a well; this is in either of the two stable states. The existence of a periodic forcing in the freshwater flux can be seen as a modification of the potential. Fig. 5 shows the potential described in (8) in three configurations, given by the three different values of the freshwater forcing that characterise the periodic forcing. Under small forcing the system will move around the initial steady-state position, and only under a much stronger disturbance will it surmount the wall and enter the other well, therefore jumping to a different regime. If the periodic forcing is too weak to cause the system to scale the potential barrier, we call the forcing sub-threshold. Under this amplitude of the forcing, the system will be trapped forever in either the weak or the strong circulation.

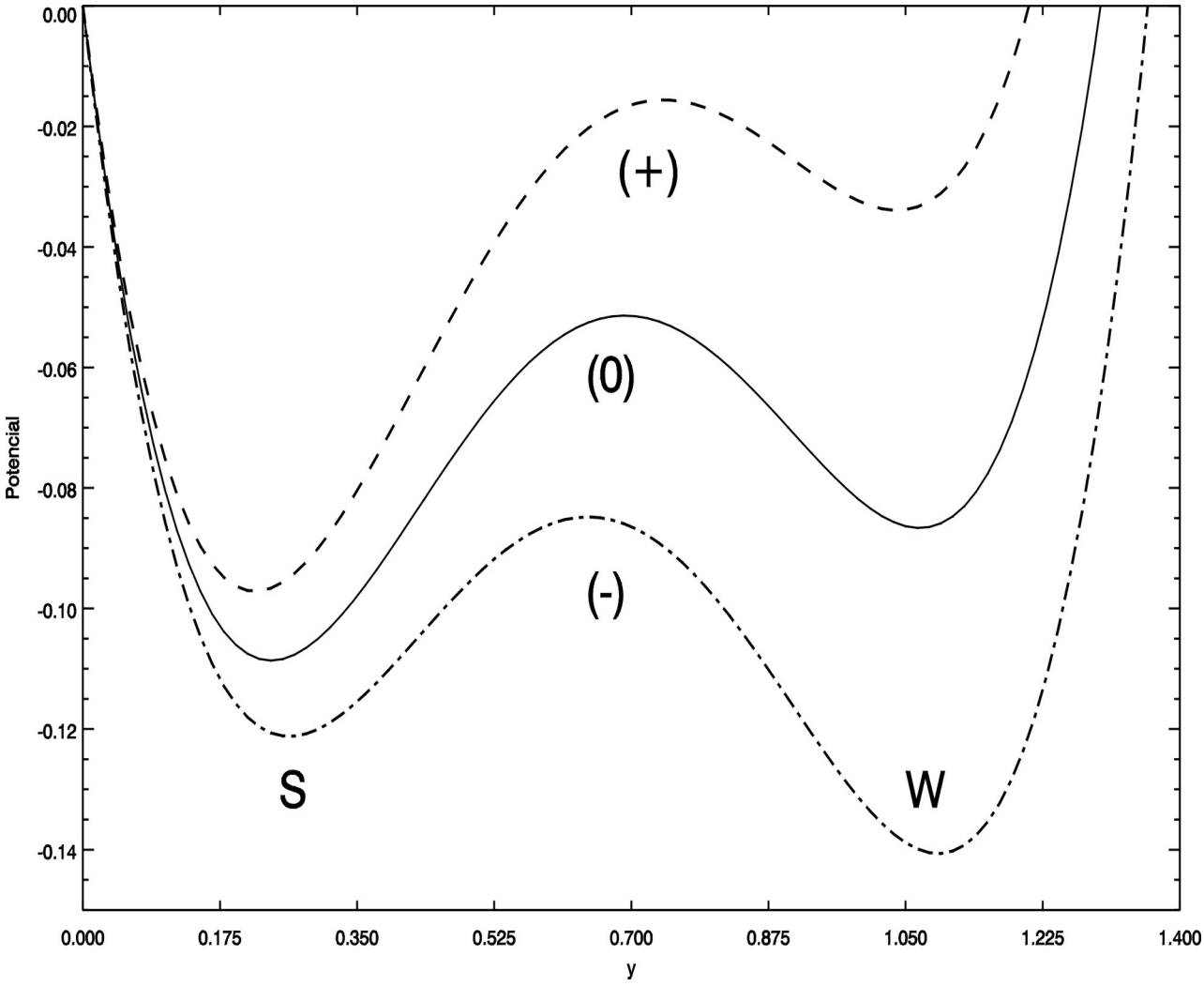

Figure 5. The potential for three different values of the freshwater forcing: (+) $p = \bar{p} + A$ (dashed line), (0) $p = \bar{p}$ (solid line) and (-) $p = \bar{p} - A$ (dot-dashed line), where $\bar{p}$=1.1 and the amplitude of the perturbation was A=0.05 (representing 4.45% of the mean freshwater flux). S denotes the strong THC solution, and W denotes the weak THC.

3.2 Mean escape times

The presence of Gaussian white noise will eventually push the system from one well to the other, with characteristic mean escape times $t_{S\to W}$ and $t_{W\to S}$. The asymmetry of the potential implies that these times are different. For small noise, the mean escape time has an exponential dependence of the ratio of the height of the potential barrier, ΔV, and the noise variance, ε, (Gardiner, 1985):

$$T \propto e^{(\Delta V/\varepsilon)}.$$

Since a periodic forcing will make the height of the potential barrier vary with time, the coexistence of a periodic forcing with noise will produce changes in the mean escape times. Following the previous notation, we will denote with $t_{(+)}$ the mean escape time when $p = \bar{p} + A$, with $t_{(-)}$ when $p = \bar{p} - A$ and with $t_{(0)}$ when $p = \bar{p}$ (see fig. 5). Then, we have the following relationship between the mean escape times in the extremes of the periodic cycle:

$$\begin{aligned} t_{(+)\,W\to S} &< t_{(0)\,W\to S} < t_{(-)\,W\to S}, \\ t_{(-)S\to W} &< t_{(0)S\to W} < t_{(+)S\to W}. \end{aligned} \tag{9}$$

Let us suppose that the period T of the forcing is such that:

$$\begin{aligned} t_{(+)\,W\to S} &<< \frac{T}{2} \qquad & t_{(-)\,W\to S} &> \frac{T}{2}, \\ t_{(-)S\to W} &<< \frac{T}{2} \qquad & t_{(+)S\to W} &> \frac{T}{2}, \end{aligned} \tag{10}$$

For a system initially in the state W, when the potential goes to the configuration (+), the probability for a jump from W to S will be higher (higher the probability smaller the mean residence time). In the same way once the system is in S, it will have a maximum transition probability when the configuration is in the (-) configuration and hence a higher probability of a jump back to W.

The system will have maximum transition probability between the two steady states with a period similar to the forcing one and in phase with it. As the jumps are induced by stochastic fluctuations, the might not take place in all the modulation periods.

Equations (10) give the range of modulation periods where the synchronisation between the noise and the forcing is such that the transitions will occur in the way described before. With a fixed forcing frequency, eqn. (10), together with the exact expression for the mean escape time (Gardiner, 1985), will yield a range of noise variance where the transition phenomena occurs. Therefore. SR can be defined as the coherence introduced by the cooperation between the input signal (periodic forcing) and the noise.

4 Simulations and results

We have performed numerical simulations of the model (4) with the freshwater forcing given by (5). Specifically, we have used the frequencies associated with the Milankovic orbital forcing. The periods for changes in the eccentricity of the orbit, in the obliquity of the earth's axis and in the timing of the seasons relative to the earth's elliptical track nearer and further from the sun are 100 kyrs, 42 kyrs, 23 kyrs and 19 kyrs, respectively.

Fig. 6a shows the dynamical evolution of the system under the combined influence of a periodic forcing with period T = 19 kyrs, amplitude A= 0.05 (this is 4.45% of the mean freshwater flux $\bar{p}$, and four times smaller than the necessary amplitude to induce transitions in the absence of noise) and random fluctuations of variance $\varepsilon = 0.022$. Jumps between the two states are clearly observed. The time series of the nondimensional transports (q) were transformed into states series in the following way: for all time where $q > 3$, the system is in the strong thermohaline overturning state and the state series takes value 1. While for the time where $q < 3$, the system is in the weak thermohaline overturning state and the state series takes value -1. The power spectrum (fig. 6c) of the state series shows a sharp peak located at the forcing frequency, riding on a broadband noise background. This indicates that the transitions between the two stable states of the two box THC preferably occur with the same periodicity as the deterministic forcing. The same effect is observed for a wide range of forcing frequencies. In particular, fig. 6b and 6d show the results for simulations with T = 42 kyrs, A= 0.05 (Corresponding to 4.45% of the mean freshwater flux) and random fluctuations of variance $\varepsilon=0.022$.

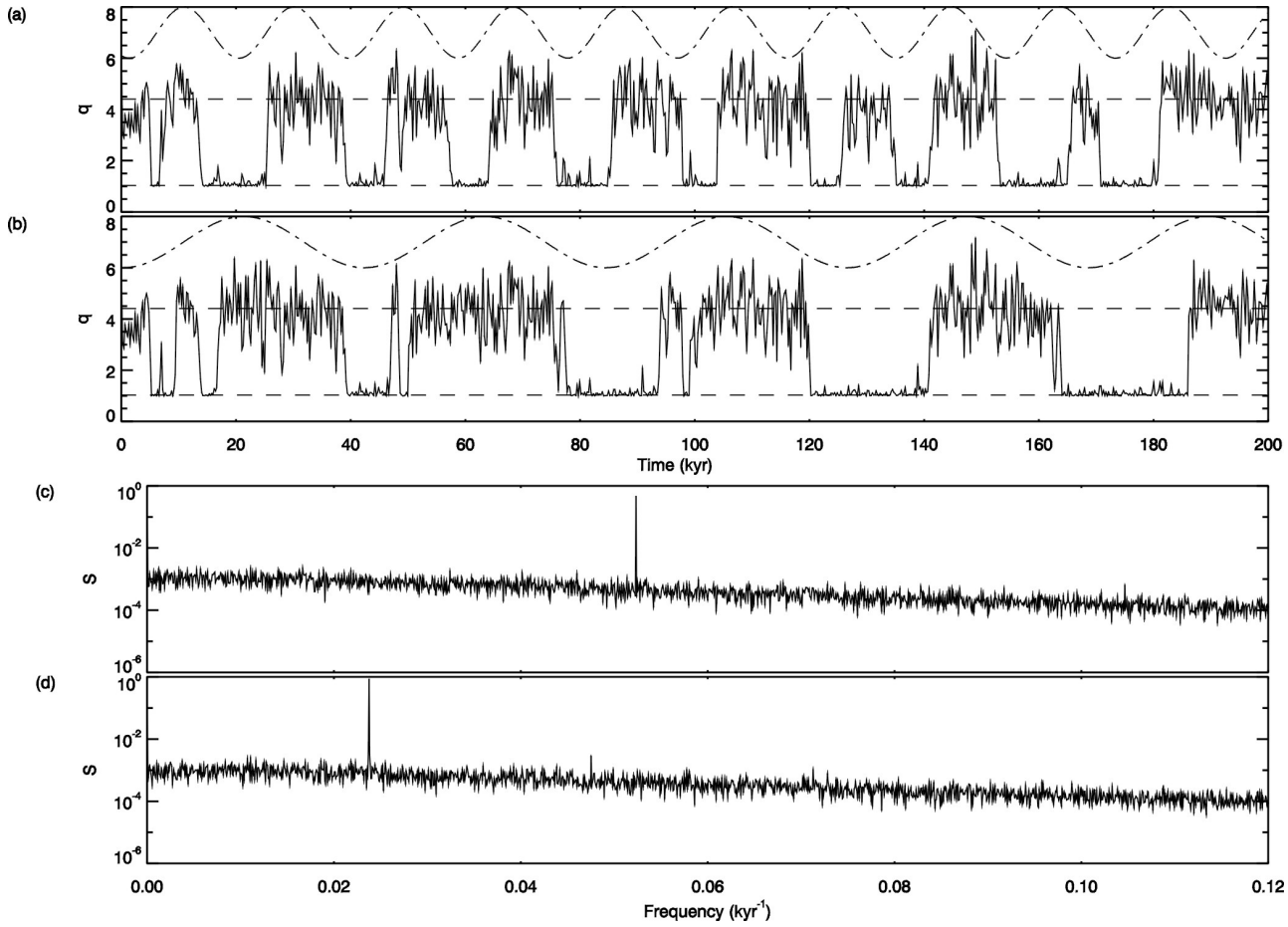

Figure 6. (a) Time series of the transport between both basins for ε = 0.022 (34 m^2 yr^{-1}), A=0.05 (4.45% of the mean freshwater forcing) and ω= 0.0727 (corresponding to a forcing period of T=19 kyrs). For reference, the dashed line indicates the position of the two stable steady states, and a dot-dashed curve in the top shows the periodic forcing (note that the amplitude and mean value of the forcing has been magnified for clarity). (c) Power spectrum computed from the time series of states of (a). (b) and (d) same as (a) and (c) except for ω= 0.0327 (T=42 kyrs).

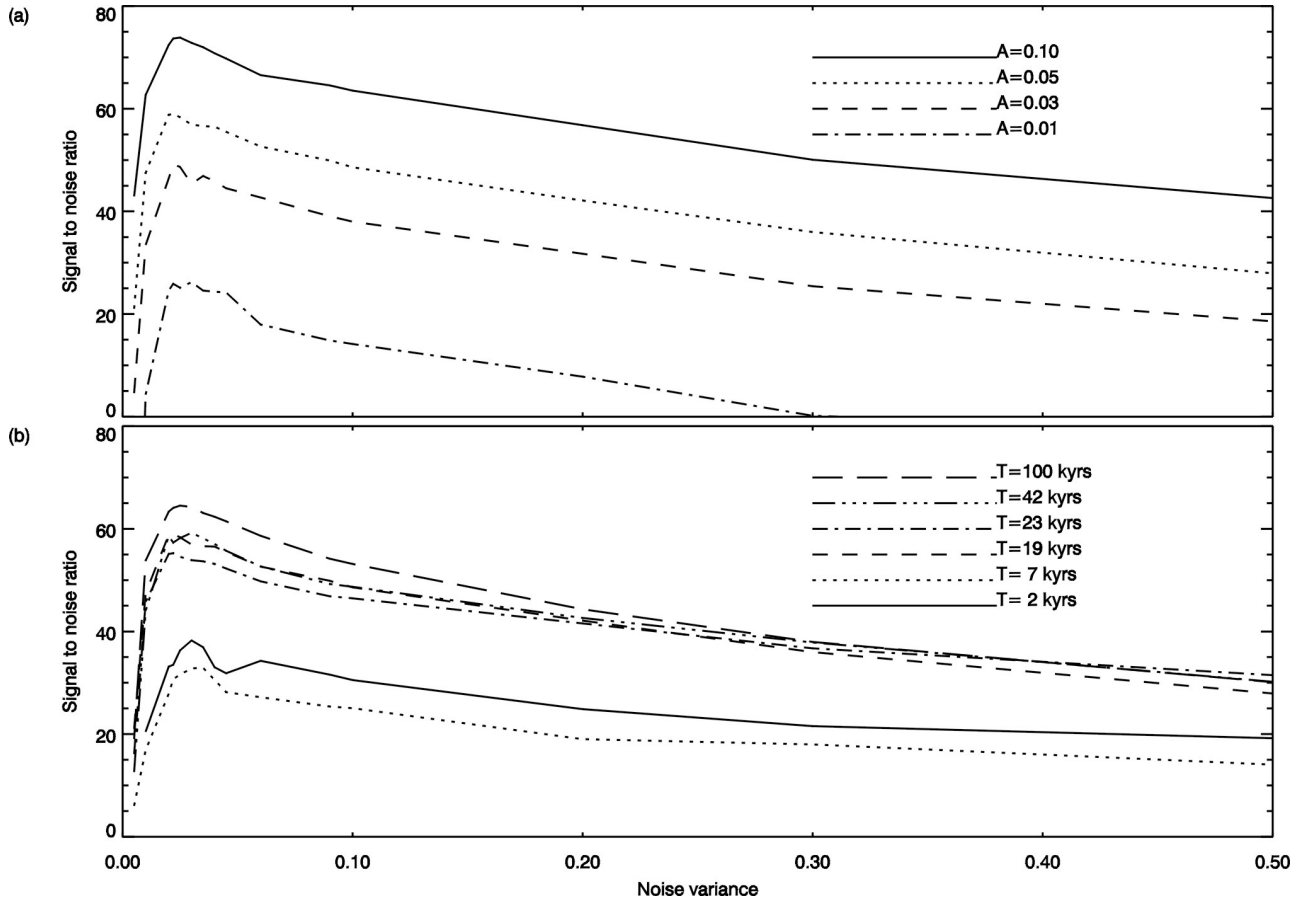

Figure 7. (a) SNR curves obtained for different amplitudes of the forcing, A=0.01, 0.03, 0.05, 0.10 (Corresponding to 0.90%, 2.72%, 4.45% and 9.09% of the mean freshwater flux, respectively). The forcing frequency is ω = 0.0727 (T=19 kyrs). (b) SNR curves obtained for different forcing periods and the same perturbation amplitude A=0.05.

An appropriate way to quantify the response of the system is by measuring the signal to noise ratio (SNR) of the power spectrum, of the state series, at the forcing frequency, S (ω_0): SNR=10 $\log_{10}$ (S (ω_0)/B), where B is the background of the spectrum. The characteristic shape of the SNR curve as a function of B is a fingerprint of the SR mechanism: SNR will increase with the noise variance, reaching a maximum value corresponding to the maximum cooperation between the signal and the noise. For large values of the noise variance, the jumps will become less synchronised with the forcing and the system's behaviour will be noise dominated, showing a slow decaying SNR curve. The computed SNR curves (fig. 7 and fig. 6c,d) show the characteristic signature of SR: a maximum in SNR takes place at an optimal value of the noise intensity which, for the parameters used in the present study it is around $\varepsilon = 0.022$.

In fig. 7, we show the computed SNR curves for different forcing periods and amplitudes. SR appears for periods ranging from 2 kyrs to 100 kyrs. Focusing on the lower limit of the perturbation amplitudes, we have found SR even for perturbations less than 1% of the mean fresh water flux. This is a much smaller number than the 16% variation in the global mean precipitation, from the modern to the glacial climate, that has been found in recent simulations (Ganopolski et al., 1998). The wide frequency range and the small amplitude required for the forcing indicates that more than an isolated phenomenon, SR in the THC could be quite common.

5 Discussion and Conclusions

A box model representing the THC has been studied under time dependent freshwater fluxes. The variability in these fluxes was represented by a weak periodic forcing and by natural environmental stochastic fluctuations. With forcing amplitudes smaller than 1% of the mean fresh water flux, the system is pushed from one stable state to the other at the frequency induced by the periodic forcing.

The idea of noise induced transitions between the different states of the THC is not new since it has been used in previous studies (among others Cessi, 1994; Weaver and Hughes, 1994). However, there are two mayor differences between our study and previous ones. First, we concentrate on the existence of a non-linear cooperative effect between the environmental noise and a weak periodic forcing that can induce transitions between the different states. Second, in our case, the induced transitions are now quasi-periodic, with the same periodicity as the forcing. As the

mechanism of SR involves the existence of fluctuations, transitions do not exactly match one by one the periods of the subthreshold periodic forcing. Consequently, periods of maximum amplitude forcing can also coexist with the North Atlantic operating in a mode opposite to the trend induced by the forcing. This cooperation is called SR, and permits transitions with lower noise strength, which are coherent with the external forcing. This occurs even when the amplitude of the periodic forcing is an order of magnitude smaller than the threshold value.

Some GCM experiments show a linear relationship between the NADW flow and the difference between the average density at two latitudinal strips. Due to the vertically averaged character of the box model, a linear relationship will yield an absolute value function of $\Delta\rho$ in eqn. (2), since the derivative of the absolute value function is singular at the origin. Hence, we have chosen a quadratic relationship between the density differences and the transport as was already proposed by Cessi and Young (1992) and Cessi (1994).

One important point not included in our model is the ice. It is well known that ice sheets can have mechanical instability that yields periodic formation of icebergs. The periodic formation and melting of icebergs could make possible the small (less that 1% of the mean freshwater forcing) amount of freshwater necessary to trigger transitions through the SR mechanism. An interesting point in this hypothesis is that the existence of climatic variability in ice-cores is much more significant during glacial periods than during the interglacial ones. This could be the consequence of SR being forced by ice-sheet instability.

The results provided here show evidence for the existence of a new extrinsic nonlinear response of the THC that might have to be considered for predicting climate change and also to understand climate variability. If, as shown, even small subthreshold periodic perturbations may be sufficient to force climate transitions when environmental fluctuations are present, then, the climate system seems to be less robust than previously considered. Recent ice core data (Bond et al, 1992, 1993; Lehman, 1993) have revealed this lack of stability of the climate system. A high resolution picture of climate dynamics during the last 250 kyrs (Dansgaard et al., 1993) has shown the existence of abrupt circum-North Atlantic climate oscillations with periods ranging from a century (Younger Dryas events) to millennial (Dansgaard Oeschger events) and 10~15 kyrs (Heinrich events (Bond et al., 1992, 1993)). The characteristics of these oscillations seem to support the idea that there was a bistable climate regime in the North Atlantic during the glacial period related to the circulation in the North Atlantic Ocean.

In summary, we have presented first evidences that a non-linear co-operative effect, SR, between the environmental noise and a weak periodic forcing in the fresh-water fluxes could induce transitions between the different stable states of the THC, with a well defined time variability. Specifically, stochastic resonance has been found in a band of frequencies, where the Milankovic orbital forcing is included. If true, SR could certainly contribute to the Earth's climate variability. Despite the simplicity of the model, the results are robust and could be observed in more complicate and representative climate numerical models.

6 Future work

The use of box models has some advantages and some disadvantages, the principal one is the impossibility to simulate one loop circulation, this is, a circulation where the waters go from the North-pole to the South-Pole in just one loop. In the present study, we have simulated the circulation in one hemisphere, the north Atlantic. The problem of using a box model trying to simulate a 'one-loop' circulation lies in the fact that an asymmetric circulation is parameterised in the box model as an unstable solution with zero transport (Q=0). The only way to avoid this problem is using, at least, a 2D (zonally averaged) model, where the asymmetric circulation is properly represented. Of course, the results are valid as the one loop circulation can be seen as a superposition of two hemispheric loops, but some interesting changes in the bifurcation diagram that appear in the 2D model could modify the frequencies and amplitudes of the noise and signal of the SR phenomena.

Another interesting point that could be investigated is the use of chaotic signal to force the ocean model. While present results have been constrained to the study of weak periodic forcings, SR can also occur under more complicate subthreshold forcings like the chaotic ones (Collins et al., 1995). Coherence between this signal and the THC would indicate the ability of the ocean to follow whatever change of the atmosphere in the presence of environmental noise.

References

Adams J.M., M. Maslin, E. Thomas, 1999: Sudden climate transitions during the Quaternary, *Progress in Physical Geography*, **23,** 1-36.

Benzi, R., A. Sutera, and A. Vulpiani, 1981: The mechanism of stochastic resonance. *J. Phys. A*, **14**, L453-457.

Benzi, R., Parisi, G., Sutera and A. Vulpiani, 1982: Stochastic resonance in climatic change. *Tellus*, **34**, 10-16.

Bond, G., H. Heinrich, W. Broecker, L. Labeyrie, J. McManus, J. Andrews, S. Huon, R. Jantschilk, S. Clasen, C. Simet, K. Tedesco, M. Klas, G. Buonani, S. Ivy, 1992: Evidence for massive discharges of icebergs into the North Atlantic ocean during the last glacial period. *Nature*, **360**, 245-249.

Bond, G., W. Broecker, S. Johnsen, J. McManus, L. Labeyrie, J. Jouzel, G. Bonani., 1993: Correlations between climate records from north Atlantic sediments and Greenland ice. *Nature*, **365**, 143-313.

Bond, G., 1995: Climate and the conveyor. *Nature*, **377**, 383-384.

Bryan, F., 1986: High-latitude salinity effects and interhemispheric thermohaline circulations, *Nature*, **323**, 301-304.

Cessi, P., and W.R. Young, 1992: Multiple equilibria in two dimensional thermohaline convection. *J. Fluid Mech*., **241**, 291-309.

Cessi, P., 1994: A simple box model of stochastically forced thermohaline flow *Journal of Physical Oceanography* **24**, 1911-1920.

Collins, J.J., C.C. Chow and T.T.Imhoff, 1995: Stochastic resonance without tuning. *Nature*, **376**, 236-238, 1995.

Dansgaard, W., S.J. Johsen, H. B. Clausen, D. Dahl-Jensen, N. S. Gundestrup, C. U. Hammer, C. S. Hvidberg, J. P. Steffensen, A. E. Sveinbjornsdottir, J. Jouzel, and G. Bond, 1993: Evidence for general instability of past climate from a 250~Kyrs ice-record. *Nature*, **364**, 218-220.

Ditlevsen, P. D., 1999: Observations of α-stable noise induced mil-lennial climate changes from ice-core record, *Geophys. Res. Lett.*, **26**, 1441-1444.

Ganopolski A., S. Rahmstorf , V. Petoukhov, M. Claussen, 1998: Simulation of modern and glacial climates with a coupled global model of intermediate complexity, *Nature*, **391,** 351-356.

Gardiner, C. W., 1985: Handbook of stochastic methods for physics, chemistry and the natural sciences. *Springer-Verlag*, 442 pp.

Ghill, M., and S. Childress, 1987: Topics in Geophysical Fluid Dynamics: Atmospheric Dynamics, Dynamo Theory, and Climate Dynamics. *Springer-Verlag*, 485 pp.

Gordon, A.L., 1986: Interocean exchange of thermohaline water. *J. Geophys. Res.*, **91**, 5037-5046.

Hughes T.M.C., and A.J. Weaver, 1994: Multiple equilibrium of an asymmetric two-basin model. *Journal of Physical Oceanography,* **24**, 619-637.

Kennet, J. P., and L. D. Scott, 1991: Abrupt deep-g, palaoceanographic changes and benthic extinction at the end of the palaeocene. *Nature*, **353**, 225-229.

Lehman, S., 1993: Ice sheets, wayward winds and sea change. *Nature*, **365**, 108-109.

Levitus, S., 1982: Climatological atlas of the world ocean, Noaa Professional paper, 13*, US Department of Commerce*, NOAA, Washington DC.

Marotzke, J., and J. Willebrand, 1991: Multiple equilibria of the global thermohaline circulation. *Journal of Physical Oceanography,* **21**, 1372-1385.

Parrilla, G., A. Lavín, H. Bryden, M. García, and R. Millard, 1994. Rising temperatures in the subtropical North Atlantic Ocean over the past 35 years. Nature **369**, 48-51.

Peixoto, J.P. and A.H. Oort, 1992: Physics of climate. American Institute of physics, 550pp.

Rahmstorf, S., 1995: Bifurcations of the Atlantic thermohaline circulation in response to changes in the hydrological cycle. *Nature*, **378**, 145-149.

Rahmstorf, S., and J. Willebrand 1995: The role of temperature feedback in stabilizing the thermohaline circulation, *Journal of Physical Oceanography,* **25**, 787-805.

Roemmich, D.H., and C. Wunsch, 1985: Two transatlantic sections: Meridional circulation and heat flux in the subtropical North Atlantic ocean. *Deep-Sea Res*., **32**, 619-664.

Rooth, C., 1982: Hydrology and ocean circulation. *Progress in Oceanography*, **11**, 131-149.

Schmitt, R. W., P. S. Bogden, and C. E., Dorman, 1989: Evaporation minus precipitation and density fluxes for the North Atlantic. *Journal of Physical Oceanograph* **19**, 1208-1221.

Stommel, H., 1961: Thermohaline convection with two stable regimes of flow. *Tellus*, **13(2)** 224-230.

Thual, O., and J.C. McWilliams, 1992: The catastrophe structure of thermohaline convection in a two-dimensional fluid model and a comparison with low-order box models. *Geophys. Astrophys. Fluid Dyn.*, **64**, 67-95.

Weaver, A. J., and T. M. C. Hughes, 1994: Rapid interglacial climate fluctuations driven by North Atlantic ocean circulation. *Nature,* **367**, 447-450.

Wiesenfeld K., and F. Moss, 1995: Stochastic resonance and the benefits of noise: from ice ages to crayfish and SQUIDs. *Nature*, **373**, 33-36.